Electronic Supplementary Material (ESI) for Biomaterials Science.
This journal is © The Royal Society of Chemistry 2023

Supplementary Information

Near Infrared Light Activatable Niosomes Loaded with Indocyanine Green and Plasmonic Gold Nanorods for Theranostic Applications

Yumnam Prince[a†], Netra Hiremath[b†], Raviraj Vankayala[a,b]

[a]*Department of Biosciences and Bioengineering, Indian Institute of Technology Jodhpur, Karwar 342030, India*

[b]*Interdisciplinary research platform, Smart Health Care, Indian Institute of Technology Jodhpur, Karwar 342030, India*

*Email: rvankayala@iitj.ac.in

†Equally contributed

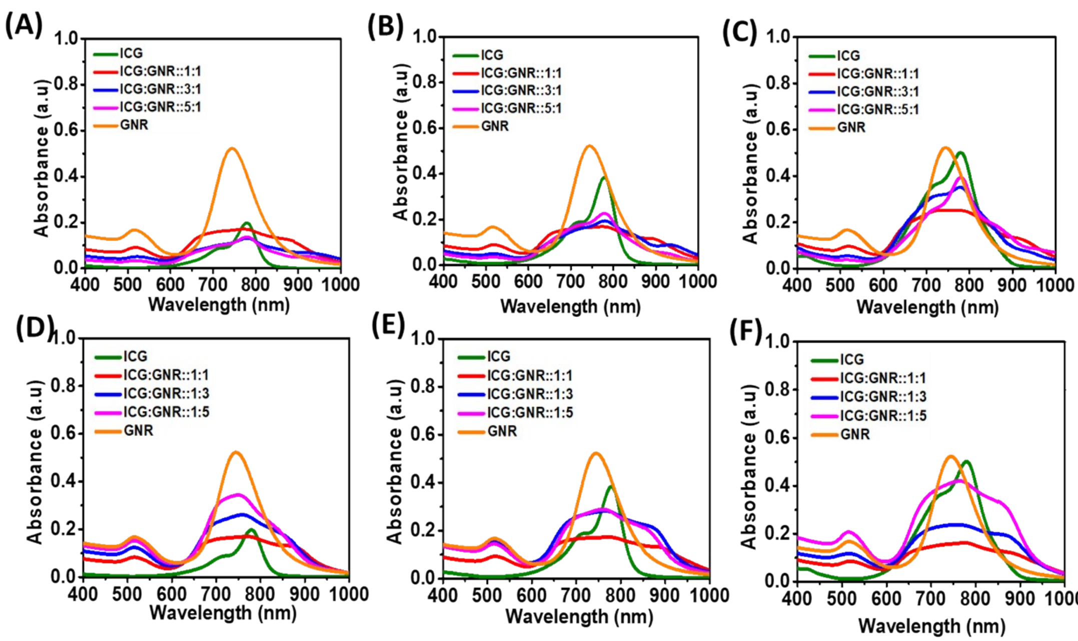

Figure S1. UV-Visible absorption spectra of (A, D) ICG (25 mM)/GNR(1.3 nM); (B, E) ICG (50 mM)/GNR(1.3 nM); (C, F) ICG (100 mM)/GNR(1.3 nM) respectively.

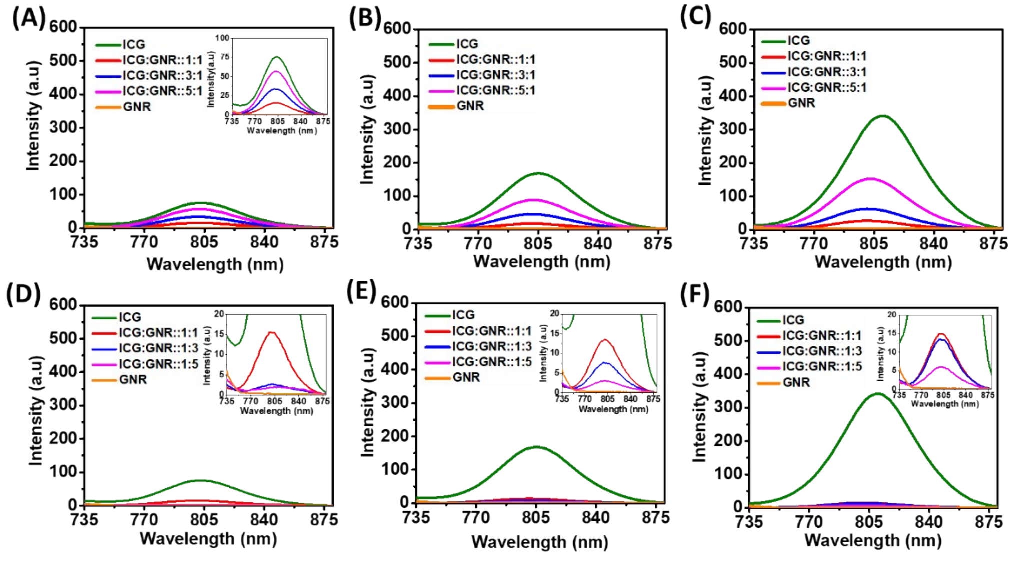

Figure S2. Fluorescence emission spectra of (A, D) ICG (25 mM)/GNR(1.3 nM); (B, E) ICG (50 mM)/GNR(1.3 nM); (C, F) ICG (100 mM)/GNR(1.3 nM). The excitation wavelength is 720 nm.

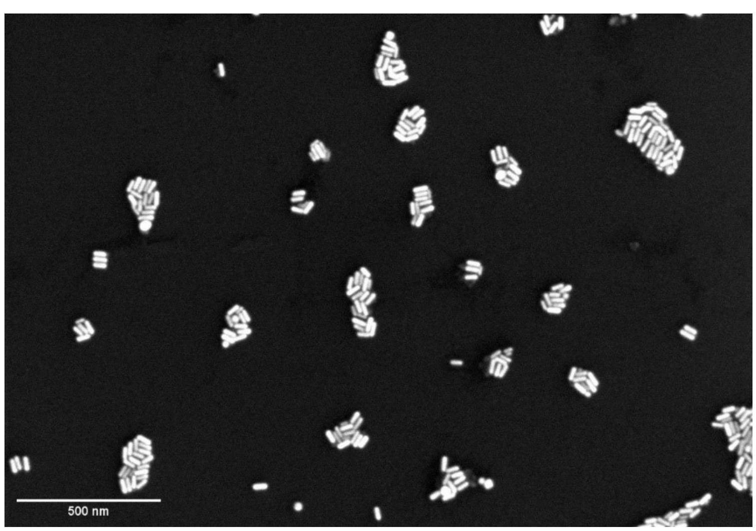

Figure S3. Scanning electron microscopy (SEM) image of plasmonic GNR.

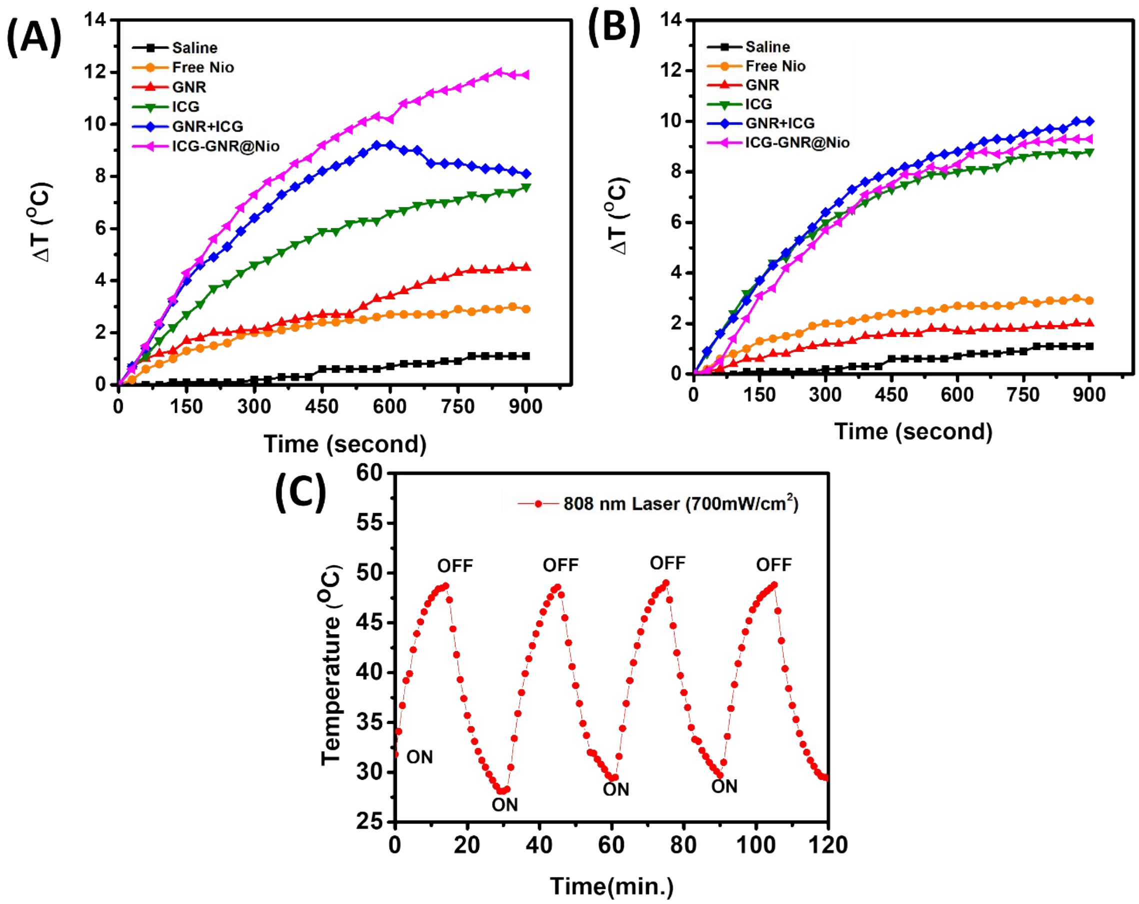

Figure S4. Photothermal temperature rise for ICG-GNR@Nio formulations. (A) exp. 1, (B) exp. 2, respectively and (C) Photostability of ICG-GNR@Nio for four ON-OFF cycles with 808 nm laser.

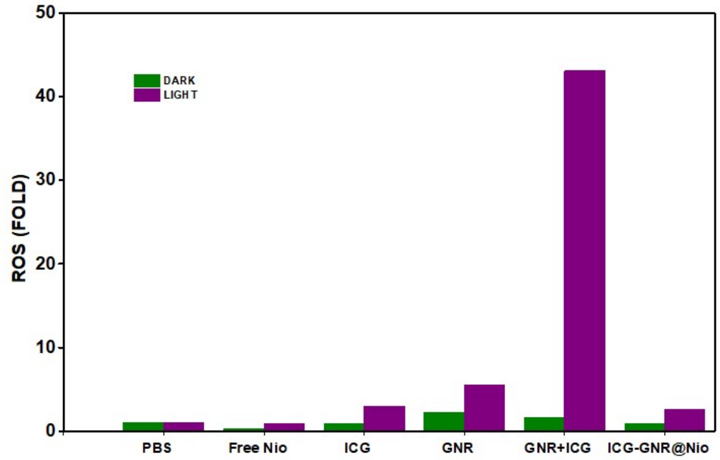

Figure S5. ROS generation with ICG-GNR under dark and photoirradiation conditions.

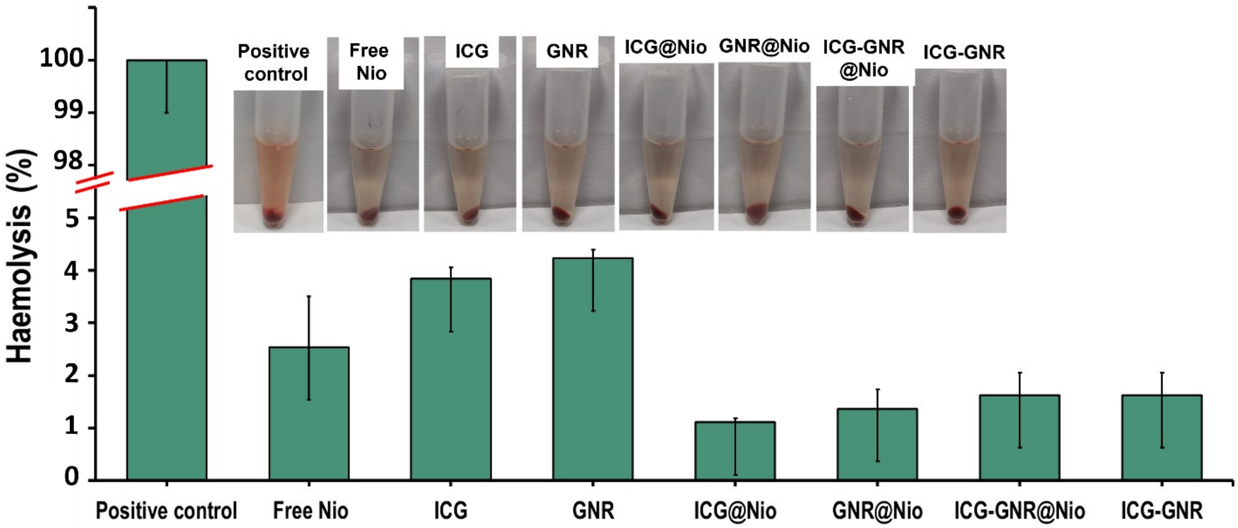

Figure S6. Hemolysis assay performed using various formulations, such as free Nio, ICG, GNR, ICG-GNR, ICG@Nio, GNR@Nio and ICG-GNR@Nio. The positive control used is nanopure water.

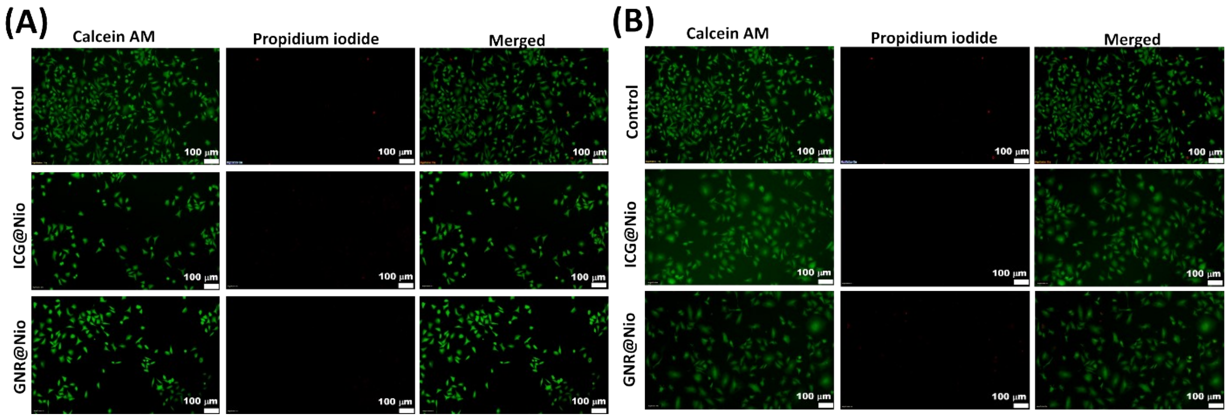

Figure S7. Fluorescence microscopy images of A549 cells treated with PBS, ICG@Nio and GNR@Nio, respectively under dark and photoirradiation conditions.

Formulation	Exp. 1	Exp. 2	Exp. 3
ICG@Nio	84%	68.6%	73.1%
ICG-GNR@Nio	80%	83.4%	87.4%

Table S1. Encapsulation efficiencies of ICG in ICG@Nio and ICG-GNR@Nio for all the three different formulations.

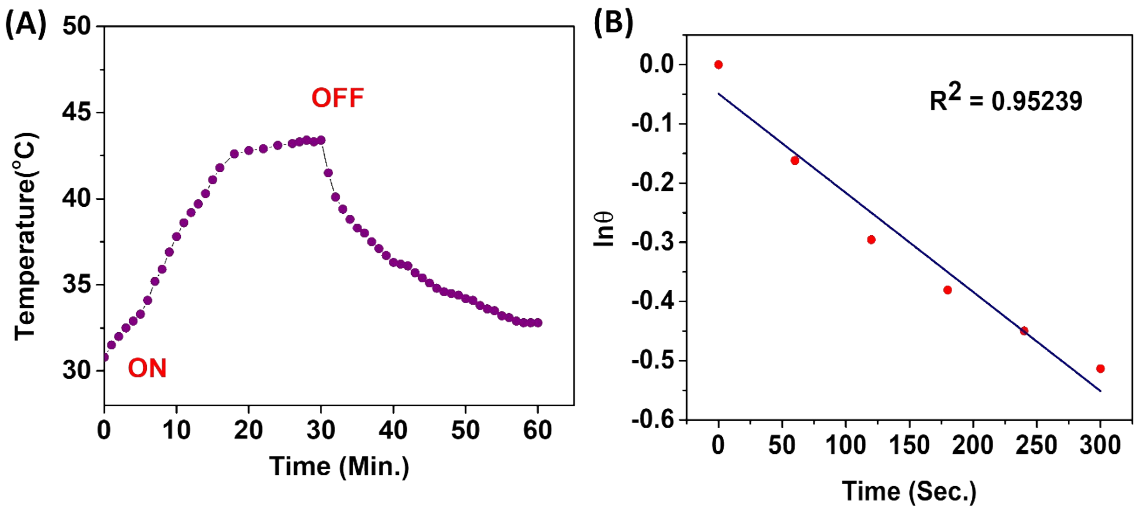

Figure S8. (a) Photothermal effect of the irradiation of the aqueous solution of the ICG-GNR@Nio Exp. 3 with the 1064 nm laser (30 min; 0.7 W/cm^2). The laser was turned off after 30 min post irradiation. (b) Linear time data versus ln(θ) obtained from the cooling period of (a).

Photothermal conversion efficiency of ICG-GNR@Nio:

The photothermal conversion efficiency of ICG-GNR@Nio (exp. 3) was calculated according to the previous method.[S1] The detailed calculation is as follows.

$$\eta = \frac{hs(T_{max} - T_0) - Q_{Dis}}{I(1 - 10^{-A1064})} \qquad (1)$$

Where *h* is the heat transfer coefficient, *S* is the surface area of the container, and the value of hS is obtained from the Eq.4 and Figure 8B. The maximum steady temperature (T_{max}) of the solution of the ICG-GNR@Nio was 43.4°C and T_0 was 30.7°C. The temperature change of the solution ($T_{max} - T_0$) was 12.7°C. The laser power *I* was 0.7 W/cm^2, the absorbance of ICG-GNR@Nio at 1064 nm (A_{1064}) was 0.95. Q_{Dis} is the heat dissipated from the light absorbed by the solvent and container and was calculated to be 7.98 mW.

In order to gain hS, a dimensionless parameter θ was introduced as follows;

$$\theta = \frac{(T_t - T_0)}{(T_{max} - T_0)} \qquad (2)$$

A sample system time constant was calculated as equation 3

$$t = -\tau_S \ln(\theta) \qquad (3)$$

According to Figure S8B, τ_S was determined and calculated to be 533 s.

$$hs = \frac{m_D C_D}{\tau_S} \qquad (4)$$

In addition, *m* is 0.3 g and *C* is 4.2 J/g·°C. Thus, according to Eq. 4, *hS* is deduced to be 3.93 mW/°C. Thus, substituting according values of each parameters to Eq. 1, the 1064 nm laser heat conversion efficiency (η) of the ICG-GNR@Nio was calculated to be 67.52%.

Supplementary References:

[S1]. X. Liu, B. Li, F. Fu, K. Xu, R. Zou, Q. Wang, B. Zhang, Z. Chen and J. Hu, *Dalt. Trans.*, 2014, **43**, 11709–11715.